Marine Ecology
MAR 2007; 28 (1) 115-130
http://dx.doi.org/10.1111/j.1439-0485.2006.00145.x

Cold-seep assemblages on a giant pockmark off West Africa: spatial patterns and environmental control

Olu – Le Roy K.[1,*], J.-C. Caprais[1], A. Fifis[1], M.-C. Fabri[1], J. Galéron[1], H. Budzinsky [2], K. Le Ménach[2], A. Khripounoff[1], H. Ondréas[3], M. Sibuet[1]

1 Département Etude des Ecosystèmes Profonds (DEEP) IFREMER Centre de Brest, BP70- 29280 PLOUZANE, France.
2 LPTC - UMR 5472 CNRS, Université Bordeaux I, 351, crs de la Libération,33405 TALENCE, France
3 Département Geosciences Marines, IFREMER Centre de Brest, BP70- 29280 PLOUZANE, France.

* : karine.olu@ifremer.fr

Abstract:

A giant pockmark colonised by dense cold-seep assemblages near 3160 m depth along the Congo-Angola margin has been surveyed by the ROV Victor 6000. The quantitative distribution of chemosynthetic communities was mapped along the dive tracks from a video study using GIS and image mosaicking. Several types of faunal assemblages, either dominated by bivalves of the families Mytilidae (*Bathymodiolus* sp.) or Vesicomyidae (*Calyptogena* sp., '*Vesicomya*' aff. *chuni*), or by Siboglinidae polychaetes (*Escarpia southwardae*) were mapped over the 800-m diameter pockmark area and sampled for fauna, water and sediment. The isotopic analyses ($\delta^{13}C$) of tissues from symbiont-bearing species were within the range typical of nutrition *via* symbiosis using methane for mussels and sulphide for vesicomyids and siboglinids. The living chemosynthetic communities were distributed on a SW-NE axis, corresponding to the expression at the sediment surface of a main buried channel providing fluids to the pockmark. The site was characterised by a more active central part in a depression with abundant carbonate concretions where high-density clusters of siboglinids and mytilids dominate. Large fields of dead and live vesicomyids with a lower mean density were observed in the external areas. The mean coverage of each of the three symbiotic taxa in these two contrasted areas was estimated from mosaic analysis and was up to 30% in the central area dominated by *E. southwardae* bushes (23%). Symbiont-bearing species distribution was consistent with methane concentrations in seawater that were generally higher in mytilid beds than in the vicinity of siboglinids and vesicomyids. A Principal Component Analysis performed on environmental factors at the ten sampling sites revealed that 37% of the observed variance in the distribution of symbiont-bearing species may be explained by variation in both methane and oxygen concentrations, while a Canonical Redundancy Analysis selected methane concentration as the only variable which explains symbiont-bearing species densities. This spatial distribution of chemosynthetic species at the pockmark scale may reflect temporal patterns of succession of both substrate and fauna, and may be related to different individual pockmarks visible on the microbathymetry mapped using ROV data.

Keywords: cold seeps, megafauna, spatial distribution, methane, symbiont-bearing species

Cold-seep assemblages on a giant pockmark off West Africa: spatial patterns and environmental control

Olu – Le Roy K.[1], J.-C. Caprais[1], , A. Fifis[1], M.-C. Fabri[1], J. Galéron[1], H. Budzinsky [2], K. Le Ménach[2], A. Khripounoff[1], H. Ondréas[3], M. Sibuet[1]

[1]Département Etude des Ecosystèmes Profonds (DEEP) IFREMER Centre de Brest, BP70- 29280 PLOUZANE, France. karine.olu@ifremer.fr. tel 33 2 98 22 46 57. Fax 33 2 98 22 47 57
[2]LPTC - UMR 5472 CNRS, Université Bordeaux I, 351, crs de la Libération,33405 TALENCE, France
[3]Département Geosciences Marines, IFREMER Centre de Brest, BP70- 29280 PLOUZANE, France.

Keywords: cold seeps, megafauna, spatial distribution, methane, symbiont-bearing species

Abstract

A giant pockmark colonised by dense cold-seep assemblages near 3160 m depth along the Congo-Angola margin has been surveyed by the ROV Victor 6000. The quantitative distribution of chemosynthetic communities was mapped along the dive tracks from a video study using GIS and image mosaicking. Several types of faunal assemblages, either dominated by bivalves of the families Mytilidae (*Bathymodiolus* sp.) or Vesicomyidae (*Calyptogena* sp., "*Vesicomya*" aff. *chuni*), or by Siboglinidae polychaetes (*Escarpia southwardae*) were mapped over the 800 m diameter pockmark area and sampled for fauna, water and sediment. The isotopic analyses ($\delta^{13}C$) of tissues from symbiont-bearing species were within the range typical of nutrition *via* symbiosis using methane for mussels and sulphide for vesicomyids and siboglinids. The living chemosynthetic communities were distributed on a SW-NE axis, corresponding to the expression at the sediment surface of a main buried channel providing fluids to the pockmark. The site was characterised by a more active central part in a depression with abundant carbonate concretions where high-density clusters of siboglinids and mytilids dominate. On the contrary, large fields of dead and live vesicomyids with a lower mean density were observed in the external areas. The mean coverage of each of the three symbiotic taxa in these two contrasted areas was estimated from mosaic analysis and was up to 30% in the central area dominated by *E. southwardae* bushes (23%). Symbiont-bearing species distribution were consistent with methane concentrations in

seawater that were generally higher in mytilid beds than in the vicinity of siboglinids and vesicomyids. A Principal Component Analysis performed on environmental factors at the ten sampling sites revealed that 37% of the observed variance in the distribution of symbiont-bearing species may be explained by variation in both methane and oxygen concentrations, while a Canonical Redundancy Analysis selected methane concentration as the only variable which explains symbiont-bearing species densities. This spatial distribution of chemosynthetic species at the pockmark scale may reflect temporal patterns of succession of both substrate and fauna, and may be related to different individual pockmarks visible on the microbathymetry mapped using ROV data.

1. *Introduction*

There is an extensive spatial heterogeneity of microbes and fauna at seeps (Levin 2005). The species richness of the symbiotic megafauna is highly variable among sites and may be explained partially by depth (Sibuet & Olu-Le Roy 2002), but is also likely to be the consequence of habitat heterogeneity. Mytilid, vesicomyid and lucinid bivalves, and siboglinid polychaetes have been described from the Louisiana slope and the Barbados prism, but at different sites. It has been suggested that their distribution may be controlled by geology, including the geometry of seeps, the pattern and volume of fluid flow, the occurrence of hydrates (MacDonald et al. 1990, Aharon 1994, MacDonald et al. 2003). Likewise, local geology can regulate the chemistry of seeps (e.g. methane and oxygen concentrations), the presence of brines, hydrocarbon composition (Sassen et al. 1994, Bergquist et al. 2005), and related faunal composition. The distribution of different Mytilidae species was also related to fluid emission intensity through mud volcanoes (Olu et al. 1996). The distribution of Vesicomyidae and other infaunal bivalves has been related to sulphide concentrations and gradients in the sediment (Barry et al. 1997, Sahling et al. 2002, Levin et al. 2003). Although several cold-seep communities have been described in Western Atlantic, the only described cold-seep site in the Eastern Atlantic is the Haakon Mosby Mud Volcano, which is covered by extensive bacterial mats and small Siboglinidae of the Monilifera group (Milkov et al. 1999, Gebruk et al. 2003). The occurrence of seeps off Mauritania is assumed from the lucky collection by fishermen of the new large *Bathymodiolus mauritanicus* Cosel 2002, and in the Gulf of Cadiz from sampling of large solemyid bivalves *Acharax* sp. and bathymodiolids on mud volcanoes (M. Cuhna pers.com.). The first seep community described

in the South East Atlantic was discovered in 2001 on a giant pockmark "REGAB" on the Gabon continental margin (Ondréas et al. 2005).

Pockmarks are sedimentary depressions caused by the seepage of fluids through the seabed. They are found world-wide along both passive and active margins, but mostly on continental shelves (Barber et al.1986, Hovland & Judd 1988). However, few cold-seep communities have been described on pockmarks. One was described on a 150m deep pockmark in the North Sea (Dando et al. 1991), but the best known example is the Bush Hill site in the Northern Gulf of Mexico, comprising a large mussel bed spread around a brine-filled pockmark at 650 m depth (MacDonald et al. 1990).

In a recent paper, thanks to a combination of video and side scan sonar mosaics collected by submarine, it has been possible to estimate the areal coverage of some cold-seep communities and the areas occupied by different components of the community at "Bush Hill" (MacDonald et al. 2003). But the quantitative distribution of seep communities has, until now, rarely been included in ecological studies. Sibuet and Olu-Le Roy (2002) proposed a classification of cold seeps with respect to the density of clusters in the active area and organisms in the clusters and the size of the active area. Variation in the density or biomass of chemosynthetic fauna at seeps has been related to the intensity of fluid flow (Henry et al. 1992; Olu et al. 1997; Sibuet and Olu-Le Roy 2002; Olu-Le Roy et al. 2004; Mau et al. 2006), and to the age of the structure or mud flow extent on mud volcanoes (Olu et al. 1997). The spatial distribution of symbiont-bearing species on mud volcanoes has also been related to the structure type (diapirs/mud pies). Like volcanoes, pockmarks also have different origins, associated with fault zones, salt diapirs or a Bottom Simulating Reflector (BSR) (Gay et al. 2003) and may differ in terms of fluid flow.

The spatial patterns of chemosynthetic communities are thus assumed to vary according to the type or activity of pockmarks. Gay et al. (2006) proposed a first model of seafloor features, including fauna distribution, related to methane flow, at the REGAB site scale, on the basis of a single video transect. However, we think that the model simplifies the spatial distribution of organisms (Olu-Le Roy, 2006).

The present ecological study combines measurements of the quantitative distribution of megafauna and environmental parameters at different spatial scales to estimate reliably the spatial distribution and coupling environmental and biological patterns at the REGAB chemosynthetic community. We mapped the community using GIS-based software and mosaicking, allowing a quantitative estimate of the extent, cover, and distribution of fauna assemblages on a giant pockmark. The distribution of the three symbiont-bearing species –

Mytilidae and Vesicomyidae bivalves and large Siboglinidae polychaetes- was analysed in the context of geological and geochemical patterns in this spatially variable cold-seep site. Biotic and abiotic variables including faunal density and biomass, substratum observations and chemical measurements in water and sediment close to the fauna, were collected simultaneously at different assemblages either dominated by Mytilidae, Vesicomyidae or Siboglinidae, in order to compare different micro-environments and the response of the chemosynthetic fauna. The major interest of this pockmark is the unusual occurrence of these three symbiotic taxa, which more typically are the sole dominant taxon at seep sites, and which are often studied separately regarding to their biotopes.

2. *Materials and methods*

2.1 Study site and symbiont-bearing species

The 800 m wide, 15 to 20 m deep pockmark REGAB was first observed as a dark spot on multibeam imagery where it appeared as a circular-shaped pockmark, apparently undisturbed by bottom currents (Ondréas et al. Fig.1). This pockmark is located over the oceanic crust (Moulin et al. 2002, Ondréas et al. 2005) less than 8 km north of the Zaïre canyon (Fig. 1). It is in an area where other fluid escape features have been observed (Kasten et al. 2001, Gay et al. 2003), including another large pockmark discovered ~60 km to the north (G. Borhmann, pers. com.). The REGAB pockmark is linked to a deep channel acting as reservoir for superficial fluids (Ondréas et al. 2005) by a 300 m long rooting pipe visible on seismic profiles, along which gas escapes. Small-scale faults, which may drive fluids upward, dip towards the centre of the feature, and develop within a tulip-shaped anomaly visible on seismic profiles (Gay et al. 2006). Although a Bottom Simulating Reflector (BSR) was not observed on the profile, gas hydrates were sampled in gravity cores from the surface to a depth of 6 m in the sediment (Charlou et al. 2004) and hydrate outcrops were observed by ROV on the seabed (Figure 2). Analyses of gas hydrate samples indicate that methane is the major chemical component of the emitted fluids (Charlou et al. 2004). The shallow burial of the paleochannel (<300 mbsf) suggests a biogenic origin of the fluids, confirmed by isotopic analyses on hydrates and fluid (Charlou et al. 2004; Levaché, personal communication) and the occurrence of a hydrocarbon reservoir linked to the pockmark is unlikely. The term “pockmark” is used throughout the paper to name the whole REGAB site, which is a depression of 15-20 m depth. Nevertheless, it is composed of several individual pockmarks less than 100 m in diameter which were identified on a microbathymetric map (Ondréas et al.

2005) and REGAB can thus be considered as a “pockmark cluster”. Dense communities dominated by large symbiont-bearing species including the Vesicomyidae bivalves “*Vesicomya” aff. chuni* and *Calyptogena* n. sp. (R. von Cosel, pers. com.), the Mytilidae *Bathymodiolus* sp. aff. *boomerang* (Olu - Le Roy et al. subm.) and the Siboglinidae polychaetes *Escarpia southwardae* (Andersen et al. 2005) were observed on the pockmark. All these species are associated with symbiotic chemoautotrophic bacteria (Duperron et al. 2005; Ondreas et al. 2005).

2.2. Video survey and analysis

The REGAB pockmark was first surveyed during 2 dives of the ROV Victor 6000 (ZAIROV cruise, 2000) and five subsequent dives during the BIOZAIRE 1 and 2 cruises were dedicated to faunal communities (Fig. 3). Megafauna assemblages were primarily classified according to the dominant megafaunal species: the mytilid *Bathymodiolus* sp., the siboglinid *Escarpia southwardae*, and the vesicomyids. It was impossible to distinguish between “*Vesicomya” aff. chuni* and *Calyptogena* n. sp. using video images. The distribution of assemblages was mapped along the dive tracks from the video study of 7 ROV dives and using the Adelie extension for ArcGIS 8.0 (©ESRI) developed at Ifremer (http://www.ifremer.fr/flotte/systemes_sm/adelie/index.html). The first dive track included ten N-S transects over the pockmark, and two transects crossing the pockmark along a SW-NE axis (Fig. 3). Subsequent dives were undertaken along this SW-NE direction where the living cold-seep communities and the concretions were observed. A point on the GIS plotted each chemosynthetic fauna assemblage during the video processing. Points with similar identifications (similar taxa) separated from less than 10 m were associated, that is to say the width of the forward-viewing video image during exploration dives at about 3 m above the bottom. Because the video survey covered a large proportion of the active zone, the areas covered by each assemblage could be visualised and their surface estimated. The substratum was characterised simultaneously and classified as soft bottom or carbonate concretions.

2.3. Detailed bathymetry

The original map of the REGAB site was derived from 4 dives by Ondréas et al. (2005) using Victor positioning and depth data (the addition of vehicle elevation above the seafloor and immersion). We improved the map for this paper by adding data from 3 new dives targeting the exploration and sampling of the central active part of the site. These new data revealed the bathymetric relief of the site and allowed more detailed comparisons with the small-scale

distribution of the fauna. The map was processed using the geostatistical analyst extension of ArcGIS 8.0 (© ESRI) and the ordinary kriging method for interpolation (spherical model of a variogram).

2.4. Video mosaic analysis

Video mosaicking was used to allow the detailed analysis of faunal distributions. Two areas were selected for mosaic creation. Mosaic 1 (70 x 50 m) is located in the largest vesicomyid field at the South-West part of the pockmark (soft bottom area) and Mosaic 2 (200 x 40 m) is positioned along the SW-NE axis colonized mostly by mytilids and siboglinid bushes with a dominance of hard bottom (Fig. 3). These two boxes were covered by video imagery, using the vertically mounted Tri-CCD camera of the ROV Victor. Transects of the mosaic were reconstructed using the MATISSE system developed at Ifremer (Allais et al. 2004). This system produces geo-referenced mosaics from a video input and navigation data. Each mosaic was about 3 m wide, corresponding to the mean altitude of the ROV during the survey, and from 10 to 30 m long (500-1000 images per mosaic). 120 mosaics of 30 m² on average and 80 mosaics of about 100 m² were analysed for Mosaic 1 and 2 respectively, using ADOBE Photoshop® to draw faunal patches. SIGMA SCAN PRO® was used to estimate the patch size for faunal groups and subsequently the total coverage of each assemblage type, either dominated by *Bathymodiolus* sp., Vesicomyidae, or *Escarpia southwardae*.

2.5. Density and biomass estimations

According to the first map of assemblage distribution, eleven assemblages (or “sites”) were selected for fauna, water and sediment sampling all over the pockmark (Fig. 3 to 5). The assemblages dominated by *Bathymodiolus* sp. (M1, M2, M3) have different cluster sizes. M3 is associated with erect *Escarpia southwardae* (Fig. 5d) and M1 with recumbent ones. The selected vesicomyid clusters have different proportions of living and dead individuals and are either isolated in the active centre of the pockmark (VC, V3), in the large vesicomyid field (VA, VB, V1) or in the external, less active area (Vext). Two erect bushes of the escarpiid *E. southwardae* were sampled, one of large adult individuals about 1.5 m long (EA, Fig. 5e), and one with smaller (tubes of less than 0.5 m long), presumably juvenile individuals (EB, Fig. 5f). Bivalve density was estimated from close-up views using four laser points spaced at 23 cm from each other or known size sampling tools for surface estimation. When possible, density was averaged from several images (6 to 16) or from complete mosaics of the sampling site. Tubeworm density was estimated using close-up images of the tubes in the vertical plane,

at different levels above the seafloor for the same bush and the surface was estimated at the base of the bush, using lasers. However, it is likely that this method under-estimates siboglinid density as all the tubes in the 3D bushes could not be enumerated.

Individual wet weights were estimated from specimens collected by the ROV grab or a slurp gun and preserved in formalin, and dry weights after 48 h at 60°C. Ten individuals of various sizes of *Bathymodiolus* sp. from M1, vesicomyids from VB and V3 and E. *southwardae* from EA and EB were available. Bivalve shells and siboglinid tubes were removed before wet or dry weight determination. Wet and dry weights were positively correlated (Pearson correlation coefficient =0.98, p=0.001).

2.7 Chemical analyses in water and sediment

Fluids were sampled using the ROV water sampling pump and collected in 200 ml titanium bottles at the different sites (Table 1). A suction cannula mounted on the ROV allowed accurate sampling of water among mytilids and vesicomyids a few centimetres above the sediment-water interface ("bottom"), just above the bivalve anterior part ("top") (Fig. 5b), at the base of the escarpiid tubes and near the worm plume. Additional water samples were obtained a few decimetres above or around the vesicomyid clusters, to highlight vertical and horizontal gradients and confirm that these clusters were associated with active methane outflows. Three sampling points from the centre to the edge of the 2 m diameter-patch were obtained in the M3 mussel bed. Water pH measurements were performed on board with a pH-meter linked to a glass electrode (metrohm). Dissolved oxygen was determined by the Winkler method adapted for small volumes, with an error of 4%. Hydrogen sulphide was measured by the colorimetric method (Fonselius,1983, error of ±5%). For sulphide analyses, 5ml of $ZnCl_2$ (0.2 mole/l) was preloaded into titanium sample bottles to precipitate the sulphide in each seawater sample as zinc sulphide prior to analysis. Methane and total carbon dioxide concentrations were measured on board using the headspace technique coupled with a gas chromatograph GC (HSS-GC) equipped with thermal-conductivity detector (TCD) and a flame-ionization detector (error of 4%) (Sarradin et al. 1996).

Sediments were collected as near as possible to assemblages by push cores of 30 cm long and 5.5 cm in diameter. The sediment cores were split on board and frozen for later analysis. Dry sediment reduced in powder was analysed for total C content with the auto-analyser LECO CS-125, and organic carbon using the auto-analyser LECO WR 12 after sediment decarbonation with 6N HCl. Total hydrocarbon measurements were performed by infra- red spectrometry according to the French AFNOR norm (NF T90-114, AFNOR, 1979).

Polycyclic Aromatic Hydrocarbons (PAHs) were analysed by gas chromatography coupled with mass spectrometry (GC/MS). Oxygen profiles were performed in the sediment using an oxygen minisensor OX 100 coupled to a picoammeter (PA 2000, UNISENSE) and a micro-manipulator using a profix data acquisition software (UNISENSE). The spatial resolution of the sensor was less than 200 µm.

2.8. Multivariate analyses

A Principal component analysis (PCA) was performed on environmental factors - methane and oxygen concentrations and substratum- at the ten sampling sites (M1, M2, M3, VA, VB, VC, V3, V1, EA, EB). The substratum was binary coded for presence or absence of soft sediment and carbonate concretions. A Canonical redundancy analysis (RDA) was also run to analyse species distributions among the different sampling sites, according to environmental factors. The first matrix included the table densities of the three symbiont-bearing species at nine sampling sites and the second matrix included environmental factors at the same sampling sites. Both PCA and RDA were performed using the 'rda' function of the VEGAN R-language library and the R PACKAGE© (R Development Core Team, 2004). We used a procedure to select the environmental variables of the RDA that contribute significantly to modelling the faunal densities at the different sampling sites. This procedure was developed by S. Dray and is available in the VEGAN R-language library.

2.9. Isotopic measurements

Mytilids, vesicomyids and siboglinids from the different sites were dissected on board and the bivalve gills and mantles and the siboglinid trophosomes, obturacula and vestimenta were frozen. After vacuum lyophilisation, 23 individuals of *Bathymodiolus* sp., 9 of both species of vesicomyids and 12 adults and juveniles of E. *southwardae* were analysed in triplicate to work out the carbon and nitrogen isotopic ratios using a DELTA Plus (thermo Finnigan) isotopic mass spectrometer (LPTC, Bordeaux).

3. ***Results***

3.1. Distribution of symbiotic megafauna assemblages at the pockmark scale

Chemosynthetic assemblages were observed throughout most dive tracks in the circular area (800 m diameter) identified previously by its high acoustic backscatter in Simrad EM12 imagery (Ondréas et al. 2005) . However, most live seep fauna was concentrated along a SW-NE axis, crossing the centre of the pockmark (Fig. 6). Scattered aggregations (~1 m in

diameter) of vesicomyid clams (mostly dead) were observed in small depressions along the first dive track in the northern and the southern part of the pockmark. The “active” section of the pockmark consisted of large *Escarpia southwardae* bushes, beds of modiolid mussels (*Bathymodiolus* sp.), and clusters of vesicomyid clams. *E. southwardae* bushes formed a dense cover (up to 20 m by 30 m) and were generally associated with small concretions or carbonate pavements. *Bathymodiolus* sp. beds covering one to several square meters (up to 50 m by 60 m) were observed in small depressions, with or without visible concretions. Vesicomyids typically occurred in clusters ~1 m in diameter, and were often found in reduced black sediment at the edge of carbonate pavements. Microbial mats were also observed in this area. Mytilid beds and siboglinid bushes were only observed in the central section of the SW-NE axis, together with carbonate concretions. Mytilids were occasionally observed on the anterior end of siboglinid tubes, and siboglinids were seen in some mussel beds (Fig. 5d). Although vesicomyids were separated from mytilids as little as 1 m, both families were not observed together within a cluster. The largest vesicomyid fields covering (50 x 100 m) were located in the eastern and western margins of the active area and included live individuals and empty shells (Fig. 6). These fields, located in depressions ~100-150 m in diameter, may correspond to individual pockmarks (Ondréas et al. 2005). The most southwestern vesicomyid field where VA, VB and V1 were located was visible on the micro-bathymetry map (Fig. 4). In contrast, the central area, a roughly circular feature (from site VC to H1) showed a positive relief which was filled by methane-derived carbonate concretions surrounded by a depression. Most of the mytilid beds were observed in this area, which was also covered by a wide *E. southwardae* field. Methane was observed at several sites within the pockmark (Fig. 4 and 2). Massive hydrates were observed on the seabed (Fig. 2a), and at other places hydrate particles floating from the seafloor. Methane gas was observed bubbling from mussel beds (Fig. 2b) and adjacent to tubeworm clusters.

3.2. Quantitative distribution at small scale

Image mosaics were prepared to compare two areas. Mosaic 1 is located in a section of the large SW vesicomyid field. Mosaic 2 is in the central part of the site (Fig. 3). Figure 7 shows examples of individual mosaics, drawn up in both areas. A quantitative analysis of the transects covering Mosaic 1 (3500 m^2 =50 m * 70 m) and Mosaic 2 (8000 m^2 =200 m * 40 m) allowed comparisons of the cover and mean density of chemosynthetic metazoan species in these areas (Table 2). Aggregations with at least some live vesicomyids covered 14% of Mosaic 1 (Table 2) but aggregations in which most individuals were live (at least 80%)

covered only 2 % of the vesicomyid field. The mean density of live individuals was 51.5 ind.m^{-2} (sd= 36.7) and 10.02 ind.m^{-2} (sd=22.6) in living and "mixed" clusters respectively. Considering these estimates, the mean vesicomyid density was approximately 2.28 ind.m^{-2} for the whole mosaic area (about 8000 ind). About 30 % of the central pockmark area (Mosaic 2) was estimated to be colonized by chemosynthetic communities, including *E. southwardae* bushes (23 %), *Bathymodiolus* sp. beds (4.5 %), and living vesicomyids clusters (2 %). Carbonate concretions were visible on 16 % of the exposed surface, but were undoubtedly more extensive, since both *Escarpia* and *Bathymodiolus* require hard substratum for settlement. Inclusion of areas occupied by *Escarpia* and mytilids increases the estimated cover of concretions and pavements to 46%.

3.3. Assemblage description, density and biomass at sampling sites

Assemblages of chemosynthetic species dominated by *Bathymodiolus* sp. varied greatly in size, mussel density (Table 3) and presence of siboglinids. Siboglinids were typically large on concretions surrounding M1 and small among mussels at M3. The vesicomyid assemblages differed by their size, density and the proportion of live and dead individuals (Table 3). The EA escarpiid bush included ~30 individuals of similar (1.5 m) tube length, and EB was mostly smaller individuals 0.15 to 0.45 m long, which were presumed to be juveniles.

The highest densities of chemosynthetic taxa were found in mussel beds. Their densities were highest (958 ind.m^{-2}) at the smaller M2 assemblage without siboglinids. Lowest densities were observed at the largest M1 site (Table 3). Density was also high in some vesicomyid clusters found in the central area (VC and V3), in the external field (V1), and in adult tubeworm bushes. The highest biomass of symbiont-bearing species (about 3 kg.m² dry weight) was found in the M2 and M3 mussel beds (Table 3). A rough estimate of the mean density and biomass of symbiont-bearing species in each mosaic area was calculated by combining the percentage cover of each assemblage type with the density/biomass estimates of individual clusters. The density of symbiont-bearing species was 2.28 ind.m^{-2} and 163.2 ind.m^{-2} in Mosaic 1 and 2, respectively. Contrast was even more evident in biomass with 0.8 g.m^{-2} in the vesicomyid field and 460 g.m^{-2} in the central area.

3.4. Methane, sulphide and oxygen concentration in water

Methane levels varied both within and among assemblages, but were generally highest in mussel beds, and much lower within vesicomyid or escarpiid aggregations. Vertical gradients in methane were measured in all assemblages, as a decrease in methane from the bottom to

the top of individuals (Table 4). Horizontal gradients were also observed, with methane decreasing from the centre to the margin of vesicomyid clusters, the M3 mussel bed, and young escarpiid bush EB (Table 4). Methane concentrations were higher above living vesicomyid clusters in the centre of the pockmark (V3, VC) or within young escarpiid bush EB than in external areas (VA, VB, V1). Hydrogen sulphide concentrations in seawater were very low or undetectable. No significant anomalies or variations in carbon dioxide and pH were detected. Oxygen levels close to mytilid clusters were homogeneous, but more variable in the vicinity of vesicomyids and escarpiids inside the sediment.

3.5. Oxygen, organic carbon and hydrocarbon in the sediment

The oxygenated zone in surficial sediments was very thin (1.5 to 3.5 mm) in areas of fluid seepage. This was consistent with the high organic carbon content of surface sediments, which varied (from 2 and 6 %) close to aggregations of symbiont-bearing species, to a maximum of 5.7 % within mytilid beds (Table 4). The total hydrocarbon concentration in the upper 4 cm of sediment was very low at vesicomyid sites and was more variable at mytilid sites. Except at M1 (89 ppm) and M2 (720 ppm) these measurements did not indicate unusual hydrocarbon contents (< 70 ppm). High levels of perylene (93-97 %) identified during the analysis of PAHs by CG/MS and HPLC suggest that the hydrocarbon content is related to hopans of bacterial origin.

3.6. Relationship fauna-habitat at sampling sites

Multivariate analyses indicated methane and oxygen were the main factors explaining the distribution of each of the three symbiotic taxa among the 10 sampling sites (Fig. 8). The first two PCA axes explained 37 % of the variance observed (23% for the first axis and 14% for the second) in faunal distributions among the environmental variables included. Canonical redundancy analyses (RDA) run with the densities of the three symbiont-bearing species at each sampling site or environmental factors for the same sites suggested that methane and oxygen could control the distribution of mytilids, whereas substratum (concretions or soft sediment) seemed to influence the distribution of siboglinids and vesicomyids (Fig.8b). The first two axes explained 42 % of the variance found in fauna densities. Depending on the procedure used, it was possible to indicate methane concentrations as the only variable explaining significantly the densities of symbiont-bearing species ($p = 0.22$).

3.7 Isotopic measurements in symbiont-bearing species

Bathymodiolus sp. tissues were more depleted in $\delta^{13}C$ than other symbiont-bearing species studied. Mussels from the M2 site had significantly lighter values, particularly the gill tissues (-67.05‰) than for mussels from M1 and M3 (Kruskal Wallis test, p=0.001). Isotopic ratios for carbon also varied slightly among mytilid tissues (p=0.11). $\delta^{13}C$ in mytilid gills was significantly heavier than mantle tissues only at M2 (p=0.001). Isotopic ratios for vesicomyid tissues from V1 and V3 did not differed significantly and no distinction could be made between gills and mantle. Adult escarpiid tissues differed significantly among sites with the least depleted $\delta^{13}C$ at M1 where mytilids dominated, and the most enriched $\delta^{13}C$ at EA. Juveniles sampled at EB also differed from adults. No differences between tissues, trophosomes and vestimenta, were detected.

4. Discussion

The REGAB site is the first cold-seep site described in the South East Atlantic. It appears as a giant pockmark formed by the association of several individual pockmarks, resulting in a large area covered by a chemosynthetic community. The live chemosynthetic assemblage is located in an area of at least 80 000 m^{-2} along a N70° axis, which probably corresponds to the main buried channel providing fluids to the pockmark (Ondréas et al. 2005). Other small (~1 m diameter) secondary pockmarks can be seen throughout the structure, filled mainly with vesicomyid shell material. The spatial distribution of chemosynthetic assemblages obtained from GIS mapping at the REGAB site scale and mosaic analyses indicates clear differences in the structure (dominant species) and density of the assemblages. The central area of the pockmark is characterized by high densities of live chemosynthetic assemblages, covering 34 % of the mosaic area analysed. This area is dominated by E. *southwardae* bushes, with small depressions containing dense mytilid beds and occasional dense aggregations of vesicomyid clams. The southwestern and northeastern margins of the pockmark were dominated by large fields of vesicomyid bivalves. Although vesicomyid shell densities were high in these fields, clusters dominated by live clams were sparse. These spatial pattern was firstly related to the methane concentrations in seawater and to the substratum heterogeneity observed at the REGAB site scale (Charlou et al. 2004, Ondréas et al. 2005). In fact, methane levels measured 3-4 m above the sea-floor were highly variable (5.8 µM vs 1.1µM) with the highest concentrations in the central area.

Chemical measurements in this study were made close to chemosynthetic species and also indicate that methane is an important factor in the distribution of the symbiont-bearing species. The highest methane concentrations recorded in mytilid dominated assemblages (Table 4). Methane concentration decreased with density in mussel beds from M2 (highest density and methane) to M3 and to the least dense M1 site. The low methane concentrations at M1 could be explained by temporal variability in methane emissions. In fact, turbulent flows of solid methane hydrate particles has been suggested to explain the high heterogeneity of methane concentration in the water column above REGAB (Charlou et al. 2004). M1 also differed from the other sites by the larger the mussel bed, lower mussel density, presence of large recumbent *Escarpia* and presence of actinians. We hypothesize that the assemblage at M1 is older than M2 and M3, and now has a decreasing methane flux. Differences in biotope chemistry among several cold-seep mussel beds has also been reported for *B. childressi* in the Gulf of Mexico (Bergquist et al. 2005). Moreover dual-symbiosis mussels may thrive in a wider range of fluid chemistry than solely methanotrophic mussels, owing to their sulphide-oxidizing symbionts (Olu et al. 1996, Levin 2005). The isotopic carbon values of its tissues (about –62‰), suggesting that methanotrophy dominates the nutrition of this species, despite dual symbiosis with both methanotrophic and sulphide-oxidizing symbionts reported by Duperron et al. (2005). Assuming negligible isotopic fractionation during methanotrophy (Conway et al. 1994), isotopic values were within the range of those of methanotrophic mussels (-40 to –70‰) (Kennicutt II et al. 1992, Conway et al. 1994, MacAvoy et al. 2005) and are consistent with the methane $\delta^{13}C$ of -67 ‰ to -70 ‰ recorded in seawater from REGAB (D. Levaché, TOTAL, pers. com.). The most depleted $\delta^{13}C$ values, suggesting a higher contribution of methanotrophic symbionts, were from the M2 site mytilids where the highest methane concentrations were recorded. However no variation in the relative abundance of sulfide- or methane-oxidizers in *Bathymodiolus* sp. gills was observed among the different sites at REGAB (Duperron et al. 2005), as has been suggested for the vent mussel *Bathymodiolus azoricus* (Colaço et al. 2002; Trask and Van Dover, 1999) under variable sulphide and methane levels.

Methane levels above assemblages are a consequence of the methane flux and of the efficiency of anaerobic methane oxidation (AMO) by the microbial consortia (Boetius et al. 2000). The total density of the microbial consortia (ANME/SRB) integrated over 0-15 cm within the sediment column was twice as high at the mussel site M3 ($18x10^6$ aggregates per ml of sediment) than at vesicomyid site V1 ($9.9x\ 10^6$) or ten times than at a microbial mat ($1.6x10^6$) (Nadalig et al. 2002). Despite microbial consortia activity and methane uptake by

mytilid symbionts, methane concentration available for the fauna at the sediment-water interface was higher above mytilids than either vesicomyids or siboglinids. Fluid flow may therefore be higher in mytilid beds. The highest sediment carbon content was also measured in mussel beds, indicating high biological production in sediments.

Methane levels near chemosynthetic taxa was the unique variable among those tested which explained the densities of symbiont-bearing species at the sampling sites in the RDA analysis, taking into account 42 % of the variance. Previous studies in western Atlantic seeps suggested that the distribution of methane-dependent mussels or sponges versus sulphide-dependent species may also be controlled by flux intensities and methane concentrations (Aharon 1994, Olu et al. 1996, Olu et al. 1997). A recent study of chemosynthetic communities on the Costa Rica margin suggested that mytilids were associated to high fluid flow rates than vesicomyids (Mau et al. 2006). MacDonald et al. (2003) indicated the occurrence of mytilids and hydrate outcrops in small areas affected by a rapid gas flux while tubeworm distribution is much more scattered. By contrast, long fluid flow duration or relict seeps may favour vesicomyids or siboglinids (Sassen et al. 1994).

Although vesicomyids were found in areas with low methane concentrations, they are not entirely independent of methane fluxes. Methane levels decreased from the centre to the outside of vesicomyid clusters, and generally increased with vesicomyid density (Tables 3, 4). Methane concentrations measured at the adult *Escarpia* bush (site EA) were low, but methane levels may be variable in both time and space. Methane bubbles were observed on video in some bushes. Higher methane levels were measured in young colonies than in adult ones but carbonate formation may slow methane flux through the sediment. Such a decrease of reduced compound levels with age or size of siboglinids has been already suggested by Julian et al. (1999) for interstitial sulphide concentrations beneath aggregations. Bergquist et al. (2003) also reported that, despite high variability within individual aggregations, sulphide is commonly present in the water surrounding the tubes of younger aggregations but is rare around the tubes of older aggregations.

Sulphide as a second energy source is also likely to play a great role in the control of sulphide-dependent symbiont-bearing species taking sulphide up from sediment pore-water, as shown for vesicomyids at other sites (Sahling et al. 2002; Levin et al. 2003). Siboglinid distributions must also be influenced by sulphide concentrations in the sediment owing to their sulphide-oxidising symbionts. These obligate symbiont-bearing species may live decades without active methane fluxes, thanks to sulphide accumulation in the sediment

(Bergquist et al. 2002). On the Haakon Mosby Mud Volcano, anaerobic oxidation of methane and sulphide production occurs only in older mud flows, and not in recent ones affected by the highest methane fluxes that preclude sulphate penetration in the upper sediment column (de Beer et al. 2006, Niemann et al. 2006). High methane fluxes may thus not favour settlement of vesicomyids or siboglinids.

As shown by the distribution of the symbiotic taxa at the REGAB site scale and results of the rda analysis, substratum is also likely to play a role in the structure of these communities. Vesicomyids are excluded from areas dominated by carbonate concretions that are favourable for siboglinids and mytilids, which require a hard substratum for larval settlement. However, the range of substratum inhabited by the mytilid *Bathymodiolus* sp. was wider than for *E. southwardae*. A better knowledge of the distribution of small size concretions and pavements under the sediment surface should help to assess the relative role of substratum, compared to methane fluxes, in the structuring the REGAB community.

5. Conclusion

The 800 m-diameter giant pockmark REGAB is characterized by high spatial variability in the structure of chemosynthetic communities, with different assemblages dominated by three key symbiotic taxa (Mytilidae, Vesicomyidae, and Siboglinidae). Although mytilids were only observed in the centre of the pockmark, this area is dominated by invertebrates with sulphide-oxidizing symbionts, and thus, does not support the preliminary hypotheses given by Gay et al (2006) model. Spatial variation in faunal structure is linked to the wide range in environmental conditions at the pockmark scale and also highlights small-scale habitat heterogeneity. The substratum is variable, ranging from areas of soft sediment to large carbonate pavements. Methane fluxes, characterized by methane concentrations a few meters above the seafloor (Charlou et al. 2004) and close to the fauna (this paper) are also highly variable. Methane levels at the sediment water interface appear as one of the key factors that regulate the distribution of each of the three dominate taxa comprising the chemosynthetic assemblages at the REGAB site.

The distribution of living fauna may also underline the variable activity of several individual pockmarks. The REGAB site appears to be a “pockmark” cluster, composed of pockmarks at different stages of activity and successional status as observed for mud volcanoes (Neurauter & Roberts 1994). The spatial variability of the fauna may also reflect temporal variability in the environmental conditions, as well as biotic interactions, e.g. competition between

dominant symbiont-bearing species. As suggested by Levin (2005), further coordinated studies at seeps with *in situ* multidisciplinary measurements over extended periods are required in order to understand the biological response to the spatial and temporal high variability in fluid flow and attendant microbial activities.

The REGAB chemosynthetic community is also inhabited by non symbiotic mega-and macrofauna, particularly Alvinocaridae shrimps (Komai and Segonzac 2005), Synaptidae holothurians and several gastropods. These seep- associated megafaunal taxa are relatively constant between assemblage types with dominance of shrimps and gastropods (Olu-Le Roy et al. 2005). However, some differences appeared in isotopic signatures of several species that could be related to differences in habitat or assemblage type.

Acknowledgments

Many thanks to the crew of the N.O. L'Atalante and VICTOR 6000 team. ZAIROV cruise (Chief scientist H. Ondréas) was the last cruise of the ZAIANGO program supported by the TOTAL oil company and Ifremer (P.I. Bruno Savoye, Ifremer). BIOZAIRE 1 & 2 cruises were partially funded by TOTAL company (BIOZAIRE program, P.I. M. Sibuet, Ifremer). Rudo von Cosel's expertise on bivalves was essential. We are indebted to D. Levaché, TOTAL for methane isotopic measurements, Philippe Crassous for sediment carbon content measurements. We are indebted to the two anonymous reviewers and to Lisa Levin and Jim Barry, editors, for their helpful comments on the manuscript.

References

Aharon P (1994) Geology and biology of modern and ancient submarine hydrocarbon seeps and vents: An introduction. Geo-Marine Letters 14:69-73

Allais A-G, Borgetto M, Opderbecke J, Pessel N, Rigaud V (2004) Seabed Video Mosaicking with MATISSE: A Technical Overview and Cruise Results. Proc. of 14th International Offshore and Polar Engineering Conference, ISOPE-2004, vol. 2 pp 417-421, Toulon, France, 23-28 Mai 2004.

Andersen AC, Hourdez S, Marie B, Jollivet D, Lallier FH, Sibuet M (2005) Escarpia southwardae sp. nov., a new species of vestimentiferan tubeworm (Annelida, Siboglinidae) from West African cold seeps. Canadian Journal of Zoology 82:980-999

Barber AJ, Tjokrosapoetro S, Charlton TR (1986) Mud volcanoes, shale diapirs, wrench faults, and melanges in accretionary complexes, Eastern Indonesia. American Association of Petroleum Geologists Bulletin 70:1729-1741

Barry JP, Kochevar RE, Baxter CH (1997) The influence of pore-water chemistry and physiology in the distribution of vesicomyid clams at cold seeps in Monterey Bay: implications for patterns of chemosynthetic community organization. Limnology and Oceanography 42:318-328

Bergquist DC, Fleckenstein C, Knisel J, Begley B, MacDonald IR, Fisher CR (2005) Variations in seep mussel bed communities along physical and chemical environmental gradients. Marine Ecology Progress Series 293:99-108

Bergquist DC, Urcuyo IA, Fisher CR (2002) Establishment and persistence of seep vestimentiferan aggregations on the upper Louisiana slope of the Gulf of Mexico. Marine Ecology Progress Series 241:89-98

Bergquist DC, Ward T, Cordes EE, McNelis T, Howlett S, Kosoff R, Hourdez S, Carney R, Fisher CR (2003) Community structure of vestimentiferan-generated habitat islands from Gulf of Mexico cold seeps. Journal of Experimental Marine Biology and Ecology 289:197-222

Boetius, A., K. Ravenschlag, CJ. Schubert, D. Rickert, F. Widdel, A. Gieseke, R. Amann, BB. Jorgensen, U. Witte, O. Pfannkuche (2000). A marine microbial consortium apparently mediating anaerobic oxidation of methane. Nature, 407 : 623-626.

Cary C, Fisher CR, Felbeck H (1988) Mussel growth supported by methane as sole carbon and energy source. Science 240:78-80

Charlou JL, Donval JP, Fouquet Y, Ondreas H, Knoery J, Cochonat P, Levache D, Poirier Y, Jean-Baptiste P, Fourre E (2004) Physical and chemical characterization of gas hydrates and associated methane plumes in the Congo-Angola Basin. Chemical Geology 205:405

Conway NM, Kennicutt MC, Van Dover CL (1994) Stable isotopes in the study of marine chemosynthetic-based ecosystems, Vol. Blackwell scientific publications, London

Cosel Rv (2002) A new species of bathymodioline mussel (Mollusca, Bivalvia, Mytilidae) from Mauritania (West Africa), with comments on the genus *Bahymodiolus* Kenk & Wilson, 1985. Zoosystema 24:259-271

Dando PR, Austen MC, Burke RA, Jr., Kendall MA, Kennicutt II MC, Judd AG, Moore DC, O'Hara SCM, Schmaljohann R, Southward AJ (1991) Ecology of a North Sea pockmark with an active methane seep. Mar Ecol Prog Ser 70:49-63

de Beer D, Sauter E, Niemann H, Kaul N, Foucher JP, Witte U, Schlüter M, Boetius A (2006) In situ fluxes and zonation of microbial activity in surface sediments of the Hâkon Mosby mud volcano. Limnology and Oceanography 51:1315-1331

Duperron S, Nadalig T, Caprais JC, Sibuet M, Fiala-Médioni A, Amann R, Dubilier N (2005) Dual symbiosis in a Bathymodiolus sp mussel from a methane seep on the gabon continental margin (southeast Atlantic): 16S rRNA phylogeny and distribution of the symbionts in gills. Applied and Environmental Microbiology 71:1694-1700

Gay A, Lopez M, Cochonat P, Sultan N, Cauquil E, Brigaud F (2003) Sinuous pockmarks belt as indicator of a shallow buried turbiditic channel on the lower slope of the Congo Basin, West African Margin. Geol Soc Lond Spec Publ 216:173-189

Gay A, Lopez M, Ondreas H, Charlou J-L , Sermondadaz G, Cochonat P (2006) Seafloor facies related to upward methane flux within a Giant Pockmark of the Lower Congo Basin. Marine Geology 226:81-95.

Gebruk A, Krylova EM, Lein A, Vinogradov GM, Anderson E, Pimenov NV, Cherkashev GA, Crane K (2003) Methane seep community of the Hakon Mosby mud volcano (the Norvegian Sea: composition and o aspects. Sarsia 88:394-403

Hecker B (1985) Fauna from a cold sulfur-seep in the gulf of Mexico: comparison with hydrothermal vent communities and evolutionary implications. Bulletin of the Biological Society of Washington 6:465-473

Henry P, Foucher JP, Le Pichon X, Sibuet M, Kobayashi K, Tarits P, Chamot-Rooke N, Furuta T, Schultheiss P (1992) Interpretation of temperature measurements from the Kaiko-Nankai cruise: Modeling of fluid flow in clam colonies. Earth and Planetary Science Letters 109:355-371

Hovland M, Judd AG (1988) Seabed pockmarks and seepages. Impact on geology, biology and the marine environment, Vol. Graham and Trotman Limited, London

Julian D, Gaill F, Wood E, Arp AJ, Fisher CR (1999) Roots as a site of hydrogen sulfide uptake in the hydrocarbon seep vestimentiferan *Lamellibrachia* sp. The Journal of Experimental Biology 202:2245-2257

Kasten S, Hensen C, Zabel M, Ravenschlag K, Boetius A, Spiess V, Schneider RR (2001) Gas hydrates in surface sediments of the Northern Congo Fan—geochemical and microbiological characterization of the top of the gas hydrate stability zone. EUG XI, Strasbourg, p 1855

Komai T, Segonzac M (2005) A revision of the genus *Alvinocaris* Williams and Chace (Crustacea: Decapoda: Caridea: Alvinocaridea), with descriptions of a new genus and a new species of *Alvinocaris*. Journal of Natural History 39:1111-1175

Levin LA (2005) Ecology of cold seep sediments: interactions of fauna with flow, chemistry and microbes. Oceanography and Marine Biology Annual Review 43:1-46

Levin LA, Ziebis W, Mendoza GF, Growney VA, Tryon MD, Mahn C, Gieskes JM, Rathburn AE (2003) Spatial heterogeneity of macrofauna at northern California methane seeps: influence of sulphide concentration and fluid flow. MEPS 265:123-139

MacAvoy SE, Fisher CR, Carney RS, Macko SA (2005) Nutritional associations among fauna at hydrocarbon seep communities in the Gulf of Mexico. Marine Ecology Progress Series 292:51-60

MacDonald IR, Guinasso NL, Jr., Reilly JF, Brooks JM, Callender WR, Gabrielle SG (1990) Gulf of Mexico hydrocarbon seep communities: VI. Patterns in community structure and habitat. Geo-Mar Lett 10:244-252

MacDonald IR, Sager WW, Peccini MB (2003) Gas hydrate and chemosynthetic biota in mounded bathymetry at mid-slope hydrocarbon seeps: Northern Gulf of Mexico. Marine Geology 198:133-158

Mau S, Sahling H, Rehder G, Suess E, Linke P, Soeding E (2006) Estimates of methane output from mud extrusions at the erosive convergent margin off Costa Rica. Marine Geology 225:129-144

Milkov A, Vogt P, Cherkashev G, Ginsburg G, Chernova N, Andriashev A (1999) Sea-floor terrains of Hakon Mosby Mud Volcano as surveyed by deep-tow video and still photography. Geo-marine Letters 19:38-47

Moulin M, Contrucci I, Olivet JL, Aslanian D, Géli L, Sibuet J, Nouze H, Réhault J, Unternehr P (2002) Deep structures of the Angola margin. In: Abstracts of the volume conference of European geophysical society, European Geophysical Society Conference. 21-26 April, Nice, p 79

Nadalig T, Caprais JC, Lösekann T, Cambon MA, Knittel K, Olu-Le Roy K, Boetius A, Sibuet M (2002) Structure and diversity of microbial communities at two methane seep sites (Gulf of Guinea) 12th Annual Goldschmitt Conference, Davos, Suisse

Neurauter TW, Roberts HH (1994) Three Generations Of Mud Volcanoes On The Louisiana Continental Slope. Geo-Marine Letters 14:120-125

Niemann H, Losekann T, de Beer D, Elvert M, Nadalig T, Knittel K, Amann R, Sauter EJ, Schluter M, Klages M, Foucher JP, Boetius A (2006) Novel microbial communities of the Haakon Mosby mud volcano and their role as a methane sink. Nature 443:854

Olu-Le Roy K (2006) Comments on the paper of Gay et al. (2006) Seafloor facies related to upward methane flux within a Giant Pockmark of the Lower Congo Basin. Marine Geology 226:81-95. Marine Geology 232:101

Olu - Le Roy K, Cosel R von, Hourdez S, Jollivet D (subm.) Do the cold-seep mussels *Bathymodilus boomerang* and *Bathymodiolus childressi* represent true amphi-atlantic species? for Deep Sea Research

Olu K, Lance S, Sibuet M, Henry P, Fiala-Medioni A, Dinet A (1997) Cold seep communities as indicators of fluid expulsion patterns through mud volcanoes seaward of the Barbados Accretionary Prism. Deep Sea Research 44:811-841

Olu-Le Roy K, Le Goff A, Fifis A, Caprais JC, Budzinsky H, Riera P, Khripounoff A, M. S (2005) Spatial distribution and nutritional patterns of megafauna on a giant pockmark in the Gulf of Guinea Third International Symposium on Hydrothermal Vent and Seep Biology, Scripps Institution of Oceanography, La Jolla (USA), September12-16, 2005: 49.

Olu-Le Roy K, Sibuet M, Fiala-Médioni A, Gofas S, Salas C, Mariotti A, Foucher JP, Woodside J (2004) Cold seep communities in the deep eastern Mediterranean Sea: composition, symbiosis and spatial distribution on mud volcanoes. Deep-Sea Research I 51:1915-1936

Olu K, Sibuet M, Harmegnies F, Foucher J-P, Fiala-Medioni A (1996) Spatial distribution of diverse cold seep communities living on various diapiric structures of the southern Barbados prism. Progress in Oceanography 38:347-376

Ondréas H, Olu K, Fouquet Y, Charlou J, Gay A, Dennielou B, Donval J, Fifis A, Nadalig T, Cochonat P, Cauquil E, Bourillet J, Moigne M, Sibuet M (2005) ROV study of a giant pockmark on the Gabon continental margin. Geo-Marine Letters 25:281

Paull CK, Hecker B, Commeau R, Freeman-Lynde RP, Neumann C, Corso WP, Golubic S, Hook JE, Sikes E, Curray J (1984) Biological communities at the Florida escarpment resemble hydrothermal vent taxa. Science 226:965-967

Sahling H, Rickert D, Lee RW, Linke P, Suess E (2002) Macrofaunal community structure and sulphide flux at gas hydrate deposits from the Cascadia convergent margin, NE Pacific. Marine Ecology Progress Series 231:121-138

Sarradin, P.-M., and J. C. Caprais. 1996. Analysis of dissolved gases by headspace sampling, gas chromatography with columns and detectors commutation. Preliminary results. Analytical Communications 33:371-373.

Sassen R, MacDonald IR, Requejo AG, Guinasso NL, Jr., Kennicutt II MC, Sweet ST, Brooks JM (1994) Organic geochemistry of sediments from chemosynthetic communities, Gulf of Mexico slope. Geo-Marine Letters 14:110-119

Sibuet M, Olu-Le Roy K (2002) Cold Seep Communities on Continental Margins: Structure and Quantitative Distribution Relative to Geological and Fluid Venting Patterns. In: G. Wefer DB, D. Hebbeln, B.B. Jorgensen, T. Van Weering (ed) Ocean Margin Systems. Springer Verlag, Berlin, p 235-251

Trask JL, Van Dover CL (1999) Site-specific and ontogenetic variations in nutrition of mussels (*Bathymodiolus* sp.) from the Lucky Strike hydrothermal vent field, Mid-Atlantic Ridge. Limnology and Oceanography 44:334-343

Figure caption:

Figure 1. Location of the REGAB site along the Gabon continental margin. The giant pockmark is located 8 km north to the Zaire canyon.

Figure 2. a. Methane hydrate outcrop, b. Gas bubbles escaping among a mussel bed.

Figure 3. Location of the 7 dive tracks and main sampled site on the REGAB site. Yellow boxes are the areas covered by mosaics.

Figure 4. Detailed bathymetry of the active central part of the REGAB site and location of the sampling sites. White dots indicate were gas bubbling was observed during the dives.

Figure 5. Assemblages dominated by symbiotic megafauna species. a. Vesicomyidae cluster V1, b. water sampling in Vesicomyidae cluster V3, c. *Bathymodiolus* sp. bed M2, d. *Bathymodiolus* bed and *Escarpia southwardae* M3, e. *E. southwardae* bush EA, f. Young *E. southwardae* bush EB.

Figure 6. Distribution map of megafauna associations dominated by mytilid or vesicomyid bivalves or by siboglinid tubeworms, along the dive tracks.

Figure 7. Two mosaics drawn using MATISSE application, in the SW vesicomyid field (MOSAIC 1, a.) and in the central area of REGAB (MOSAIC 2, b.). Video images were used to create each mosaic.

Figure 8. Ordination graphs showing the first two axes of PCA (a) and RDA (b). Arrows indicate direction of increase in environmental parameters

Tables

Table 1: Sampling sites (O.C.: Organic carbon, PAHs :Polycyclic Aromatic Hydrocarbons, THcs :Total Hydrocarbons

Sampling site	Cruise	fauna/substrate	measured parameters in water	measured parameters in sediment
M1	BZ2	*Bathymodiolus* sp.	CH_4, CO_2, O_2, pH, H_2S	O.C., O_2 profile, PAHs, THcs
M2	BZ2	*Bathymodiolus* sp.	CH_4, CO_2, O_2, pH, H_2S	O.C., THcs
M3	BZ2	*Bathymodiolus* sp.	CH_4, CO_2, O_2, pH, H_2S	O.C., O_2 profile, THcs
VA	BZ1	Vesicomyidae (living)	CH_4, CO_2, O_2, pH	O.C.
VB	BZ1	Vesicomyidae (dead)	CH_4, CO_2, O_2, pH	
VC	BZ1	Vesicomyidae	CH_4, CO_2, O_2, pH	
V1	BZ2	Vesicomyidae	CH_4, CO_2, O_2, pH, H_2S	O.C., PAHs, THcs
V3	BZ2	Vesicomyidae	CH_4, CO_2, O_2, pH, H_2S	O.C., O_2 profile, PAHs THcs
EA	BZ1	Adult *Escarpia* sp.	CH_4, CO_2, O_2, pH	
EB	BZ1	Young *Escarpia* sp.	CH_4, CO_2, O_2, pH	

Table 2: Cover and mean cluster sizes of symbiont-bearing species aggregates in the mosaic areas of REGAB. For location see Fig. 4.

Mosaic	Cluster type	Area (m^{-2})	Cover (%)	Mean cluster size (sd; n) (m^2)
1	Vesicomyidae, living	73	2.1	0.6 (1.1;85)
	Vesicomyidae, living/dead	418	12	4.5 (3.5;40)
	Vesicomyidae, shells	473	13.6	4.2 (4.9; 99)
	Total living	491	14.1	1.85 (2.8;125)
	Total dead	473	13.6	4.2 (4.9; 99)
2	*Escarpia*, dense	1444	18.2	5.66 (9.1;255)
	Escarpia + *Bathymodiolus*	267	3.4	9.21 (12.5;29)
	Escarpia young	43	0.54	0.93 (1.6;45)
	Escarpia, sparse	57.6	0.73	8.23 (5.4;7)
	Escarpia, recumbent	196	2.5	5.03 (7.1;39)
	Escarpia, senescent	80	1	3.5 (9.1 ;23)
	Mytilidae, dense	333.6	4.2	3.1 (4.8 ;108)
	Mytilidae, sparse	27.6	0.35	3.06 (2.3;9)
	Mytilidae shells	27.5	0.35	1.1 (0.4;3)
	Vesicomyidae, living	28	0.35	0.83 (0.8;34)
	Vesicomyidae living/dead	157	2	2.57 (4.1;60)
	Vesicomyidae shells	140	1.8	1.83 (1.9;75)
	Total living	2358	29.8	4.3 (7.6;547)
	Total dead	443	5.65	3 (4.5;140)
	Concretions	1240	16	6.7 (9;187)

Table 3: Density and biomass of mytilid, vesicomyid clusters and siboglinid bushes sampled in the REGAB site. See Fig. 4 for location. * densities from mosaic covering the whole cluster

Site	Cluster size (m^2)	Percentage of living individuals	Mean density ($ind.m^{-2}$) (s.d.;n)		Biomass ($kg.m^{-2}$) Wet weight – Dry weight	
			Bathymodiolus sp. / Vesicomyidae	*E. southwardae*.	*Bathymodiolus* sp. / Vesicomyidae	*E. southwardae*.
M1	400	~100	591.8 (116;8)	250.0*	7.84 - 1.97	2.31 - 1.09
M2	1	~100	958.9 (283.5;6)	0	12.71 - 3.19	
M3	4	~100	870.1 (196.4 ;11)	251.1*	11.53 - 2.9	2.32 - 1.10
V1	4	>80	586.4 (109 ;16)		7.00 - 1.55	
VC	0.75	>80	607.5*		7.25 – 1.61	
V3	0.35	>80	484.5*		5.78 - 1.28	
VA	0.4	~50	173.0*		2.06 - 0.46	
Vext	0.45	~50	66.7*		0.79 – 0.17	
EA	<0.5	?		557.3 (335.5;10)		5.14- 2.43
EB	<0.25	~100		250.0 (69.7;7)		0.53- 0.18

Table 4. Chemical characteristics of the water in bivalves clusters and siboglinid bushes sampled in REGAB. Bottom samples were taken between the bivalves or at the base of the tubeworms the closest to the sediment, top samples at the anterior edge of the shells or at the level of the siboglinid plumes. Values between brackets were taken a few decimetres outside the clusters. Co.= concretion, Co. /sed= concretions surrounded by soft sediment, S. sed.= soft sediment

Sampling site	CH_4 (µM) bottom/top	CO_2 mM	H_2S µM	O_2 µM	pH	POC (%)	Substratum
M1 centre	1.6-0.7	n. e.	<0.1	240	7.7	5.755	Co.
M2 centre	33.7-23.2	n. e.	<0.1	230	7.7	3.09	Co. /sed
M3 centre	23.5-12.5	n. e.	<0.1	230	7.8	3.665	Co. /sed
M3 middle	9.4-8.7	n. e.	<0.1	233	7.8		
M3 periphery	11.8-6.3	n. e.	<0.1	230	7.8		
VA	0.99-0.46 (0.3)	2.2	n. e.	211-238	7.8	3.0	S.sed
VB(dead)	0.42 - 0.22	2.1	n. e.	175-233	7.8		S. sed.
VC	3.9-1.6	2.3	n. e.	220	7.7		S. sed.
V1	0.9-0.4	n. e.	<0.1	221	7.8	2.26	S. sed.
V3	4.4-3.4	n. e.	n. e.	236	7.8	2.23	S. sed.
EA (adult)	1.11-0.63	2,4	n. e.	218-231	7.8		Co.
EB (young)	4.45-2.43 (0.41)	2,2	n. e.	218-232	7.8		Co.

Table 5: Isotopic values of symbiont-bearing species collected at different sampling site on the REGAB pockmark. Number of measured individuals indicated in brackets. *For *Escarpia southwardae*, mean $\delta^{13}C$ and $\delta^{15}N$ calculated from the 3 tissues analysed (trophosome, vestimentum and obturaculum) are presented because no significant differences were detected among tissue types.

Species/sites	$\delta^{13}C$ (‰) Mantle	$\delta^{13}C$ (‰) Gill	$\delta^{15}N$(‰) Mantle	$\delta^{15}N$ (‰) Gill	$\delta^{13}C$(‰) Mean*	$\delta^{15}N$(‰) Mean*
Bathymodiolus sp.						
M1	-63,3±3.5 (6)	-63,7±2.1	-0,5±0.8 (6)	-0,6±0.3		
M2	-64,5±0.8 (5)	-67,0±0.8	0,3±0.5 (3)	-0,7±0.4		
M3	-63,7±1.5 (6)	-62,4±0.9	-1,9±0.9 (12)	-3,1±1.0		
Vesicomyidae sp.						
V1	-35,6±1.6 (5)	-35,7±1.1	2,9±2.0 (3)	-1,0±2.1		
V3	-36,0±0.8 (4)	-36,0±0.15	3.5±0.3 (5)	2.9±2.0		
E. southwardae						
M1					-24.2±5.5 (5)	2.5±1.6 (6)
EA (adult)					-36,22±3.3 (4)	2,9±0.6 (5)
EB (young)					-29.1±3.4 (3)	-

Fig1

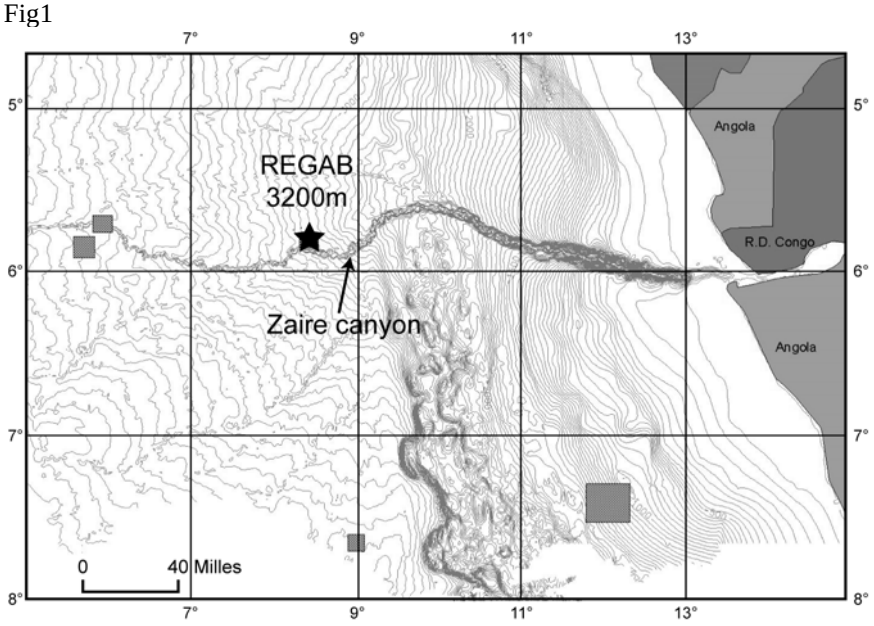

Fig2a

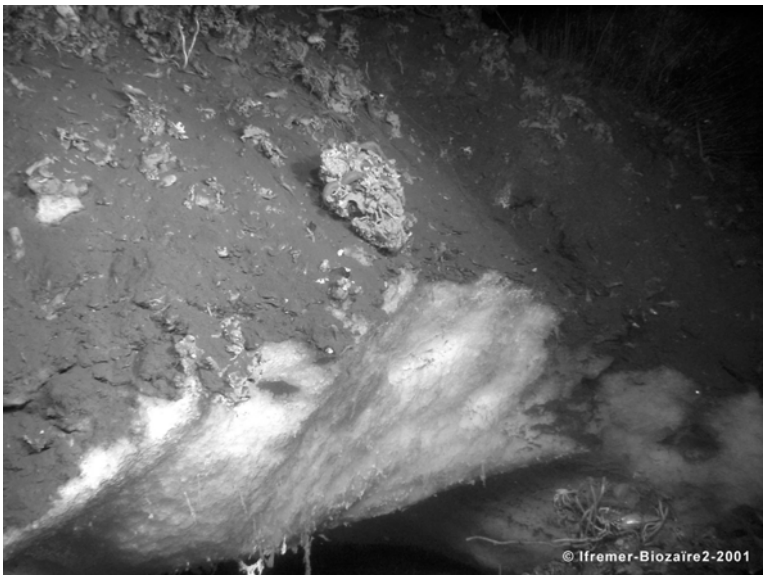

Fig 2b

Fig 3

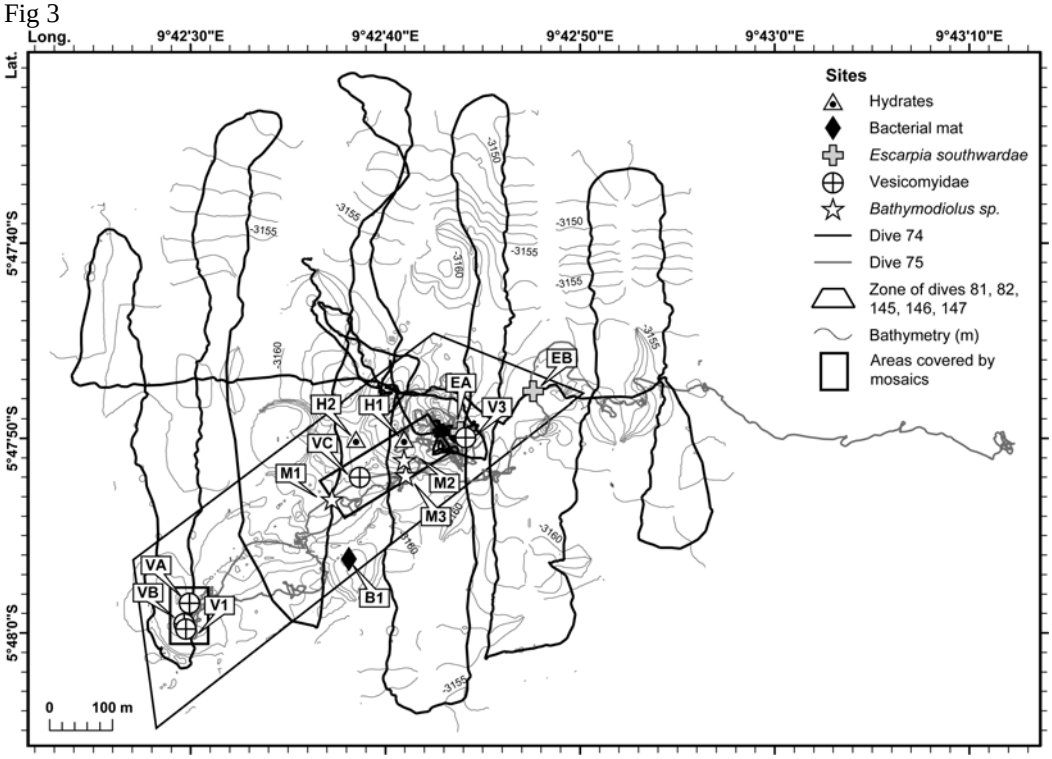
Long.
9°42'30"E
9°42'40"E
9°42'50"E
9°43'0"E
9°43'10"E
Lat.
5°47'40"S
5°47'50"S
5°48'0"S
Sites
Hydrates
Bacterial mat
Escarpia southwardae
Vesicomyidae
Bathymodiolus sp.
Dive 74
Dive 75
Zone of dives 81, 82, 145, 146, 147
Bathymetry (m)
Areas covered by mosaics
EB
EA
H2
H1
V3
VC
M1
M2
M3
VA
VB
V1
B1
0
100 m

Fig4

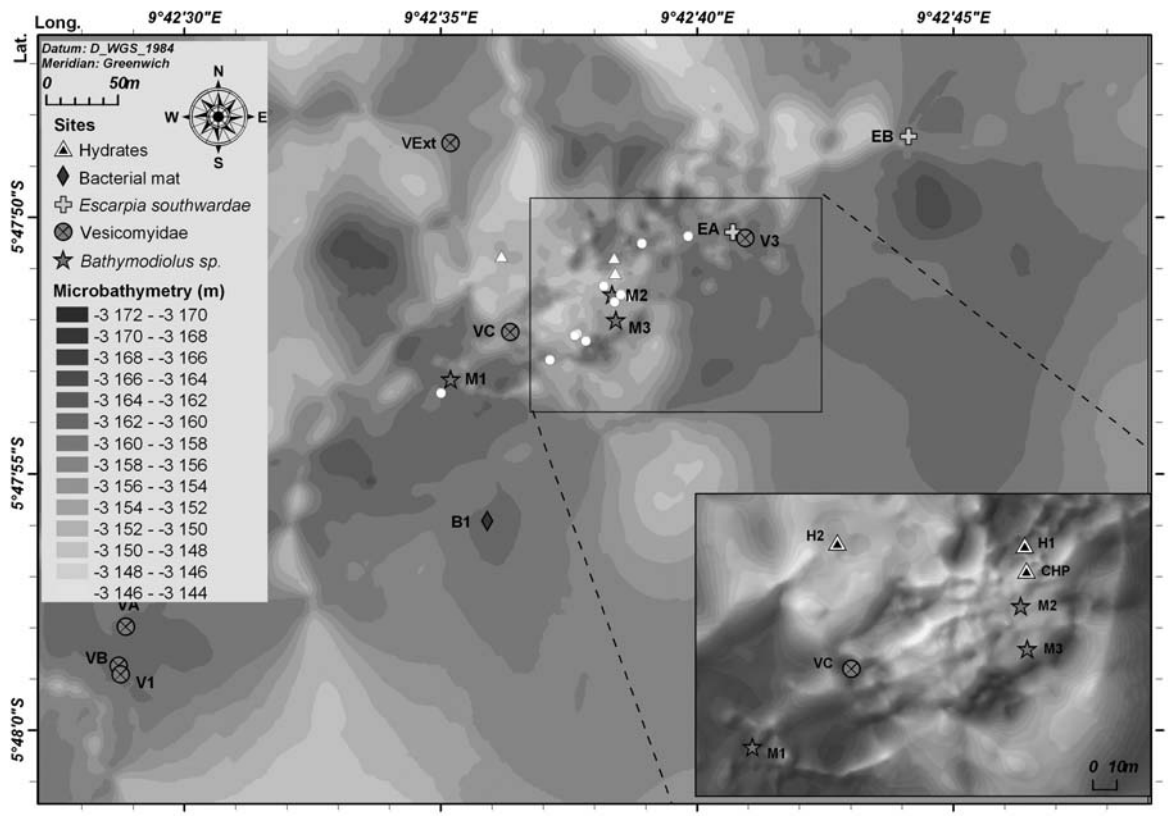
Long.
9°42'30"E
9°42'35"E
9°42'40"E
9°42'45"E
Lat.
5°47'50"S
5°47'55"S
5°48'0"S
Datum: D_WGS_1984
Meridian: Greenwich
0 50m
N
W
E
S
Sites
Hydrates
Bacterial mat
Escarpia southwardae
Vesicomyidae
Bathymodiolus sp.
Microbathymetry (m)
-3 172 - -3 170
-3 170 - -3 168
-3 168 - -3 166
-3 166 - -3 164
-3 164 - -3 162
-3 162 - -3 160
-3 160 - -3 158
-3 158 - -3 156
-3 156 - -3 154
-3 154 - -3 152
-3 152 - -3 150
-3 150 - -3 148
-3 148 - -3 146
-3 146 - -3 144
VExt
EB
EA
V3
M2
M3
VC
M1
B1
VA
VB
V1
H2
H1
CHP
M2
M3
VC
M1
0 10m

Fig 5a


© Ifremer-Biozaïre2-2001

Fig 5b

Fig 5c

Fig 5d

Fig 5e

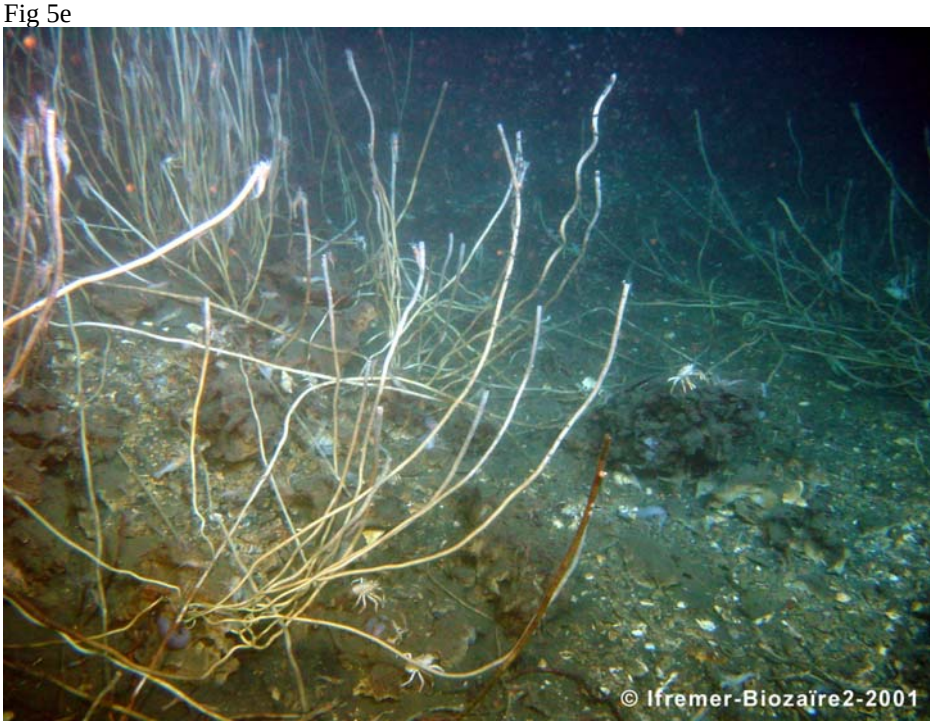

Fig 5f


© Ifremer-Biozaïre2-2001

Fig 6

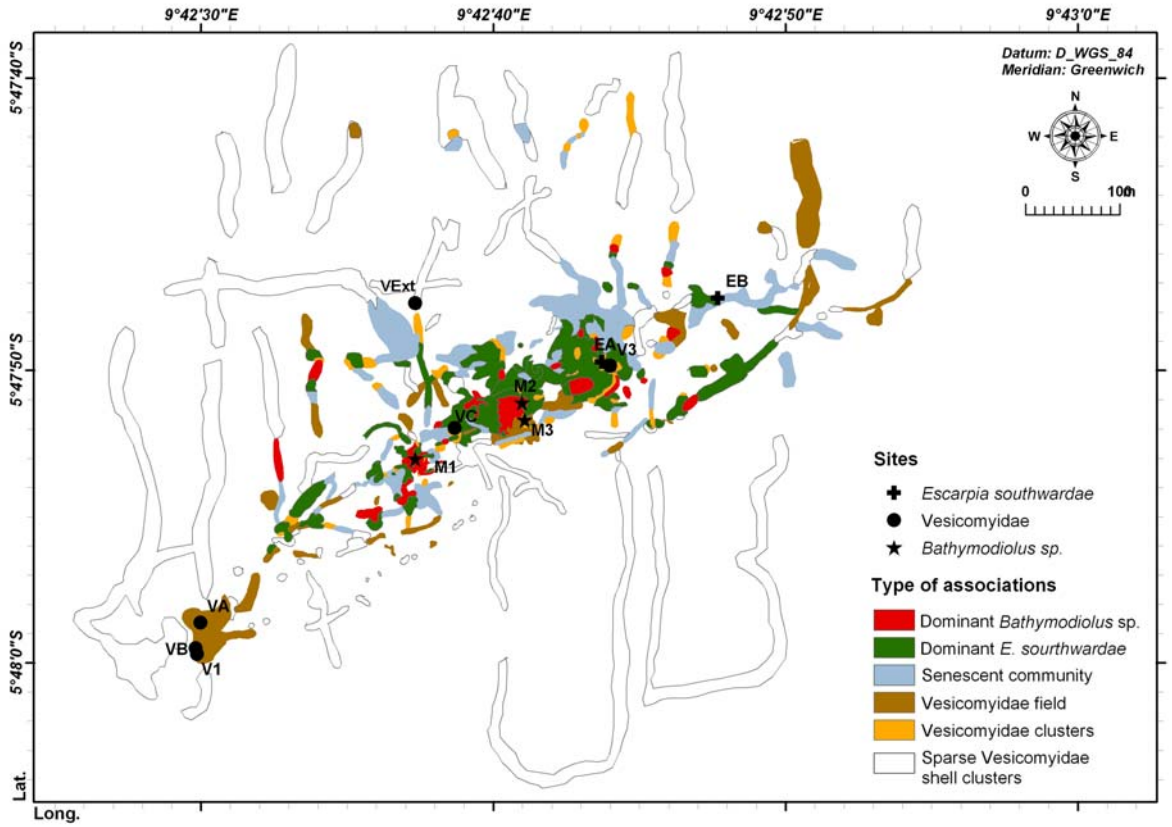
9°42'30"E
9°42'40"E
9°42'50"E
9°43'0"E
5°47'40"S
5°47'50"S
5°48'0"S
Lat.
Long.
Datum: D_WGS_84
Meridian: Greenwich
N
W
E
S
0
100m
VExt
EB
EA
V3
M2
M3
VC
M1
VA
VB
V1
Sites
Escarpia southwardae
Vesicomyidae
Bathymodiolus sp.
Type of associations
Dominant Bathymodiolus sp.
Dominant E. sourthwardae
Senescent community
Vesicomyidae field
Vesicomyidae clusters
Sparse Vesicomyidae shell clusters

Fig 7a

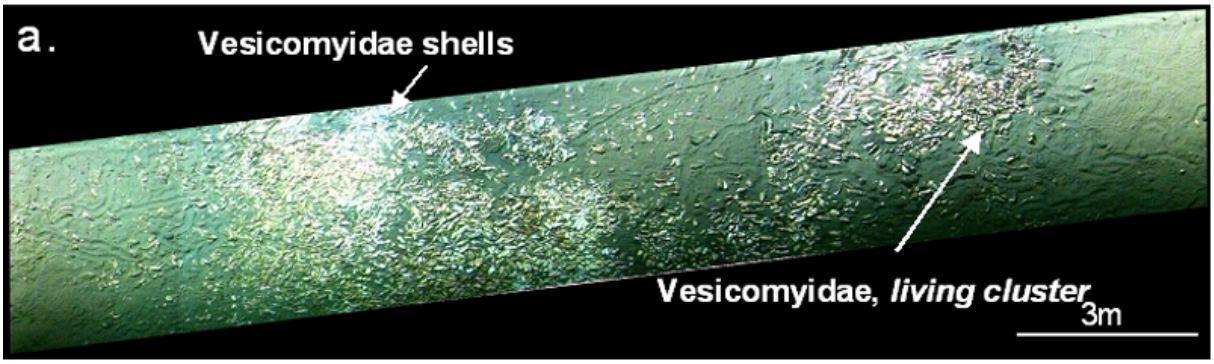

Fig 7a

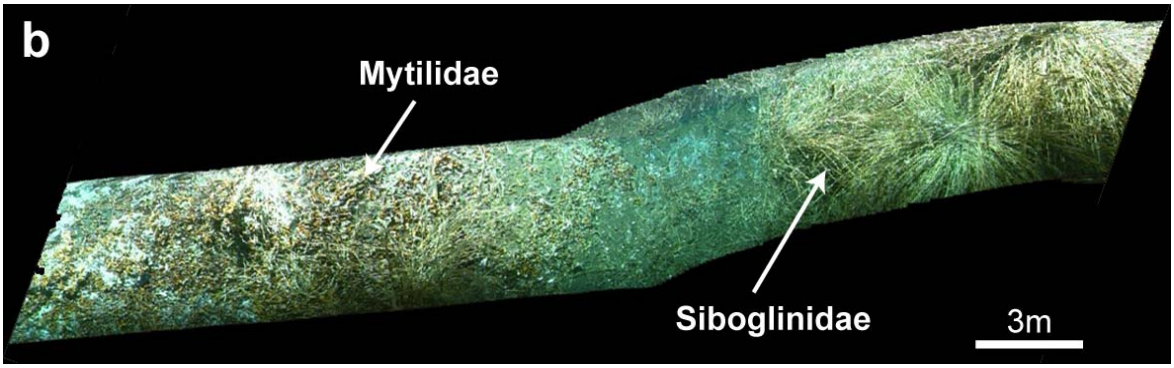

Fig 7b

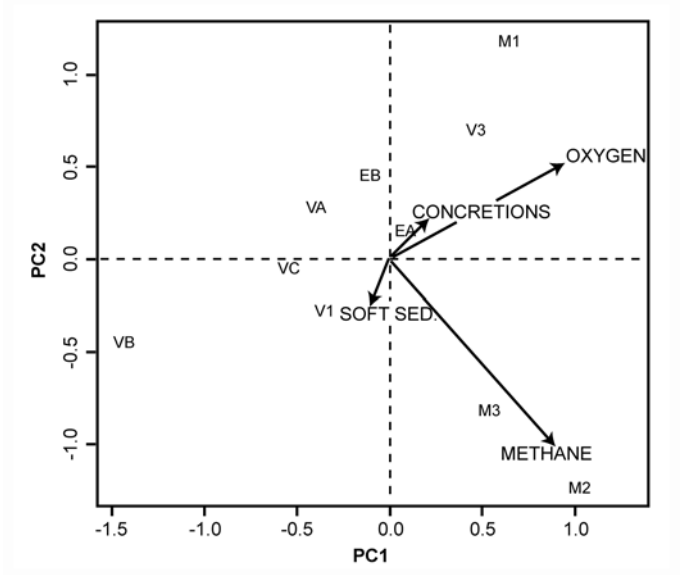

Fig 8a

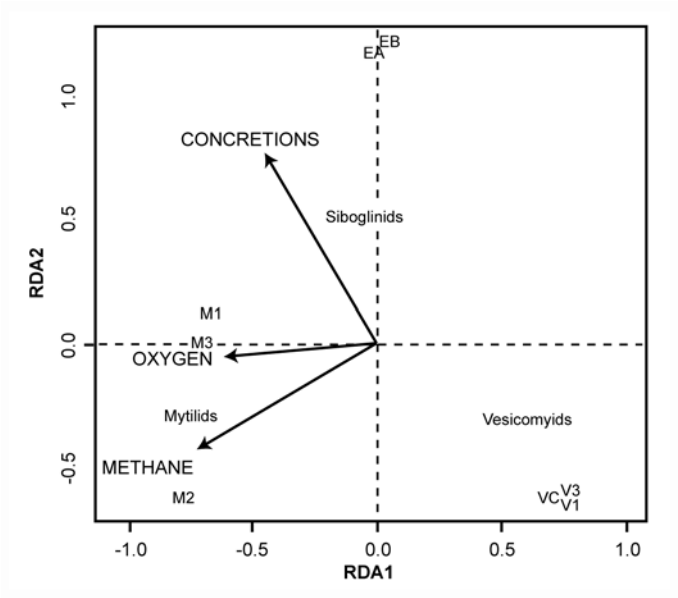
EB
EA
CONCRETIONS
Siboglinids
M1
M3
OXYGEN
Mytilids
Vesicomyids
METHANE
M2
VC
V3
V1
RDA2
RDA1
1.0
0.5
0.0
-0.5
-1.0
-0.5
0.0
0.5
1.0
Fig 8b